

Band structure calculations for $\text{Ba}_6\text{Ge}_{25}$ and $\text{Ba}_4\text{Na}_2\text{Ge}_{25}$ clathrates

Ivica Zerec, Alexander Yaresko, Peter Thalmeier, and Yuri Grin

Max Planck Institute for Chemical Physics of Solids, D-01187 Dresden, Germany

(Dated: October 24, 2018)

Electronic band structures for $\text{Ba}_6\text{Ge}_{25}$ and $\text{Ba}_4\text{Na}_2\text{Ge}_{25}$ clathrates are calculated using linear muffin-tin orbital method within the local density approximation. It is found that barium states strongly contribute to the density of states at the Fermi level and thus can influence the transport properties of the compounds. A sharp peak of the density of states is found just at the Fermi level. It is also shown that the shifting of barium atoms toward experimentally deduced split positions in $\text{Ba}_6\text{Ge}_{25}$ produces a splitting of this peak which may be interpreted as a band Jahn-Teller effect. If the locking of the barium atoms at the observed structural phase transition is assumed, this reduction of the density of states at the Fermi level can account for the experimentally observed decrease of the magnetic susceptibility and electrical resistivity at the phase transition, and the values of density of states are in agreement with low temperature specific heat measurements and variation of superconducting transition temperature with pressure.

PACS numbers: 71.20.-b, 71.20.Tx

I. INTRODUCTION

$\text{Ba}_6\text{Ge}_{25}$ clathrate^{1,2,3} attracted considerable scientific interest and initiated an intense experimental activity because of its rich physical properties. This class of compounds is investigated primarily because of their thermoelectric properties.⁴ The concept of PGEC, phonon-glass electron-crystal, was introduced. Massive alkali and alkali-earth metal atoms are expected to rattle in oversized cages usually formed by Si, Ge or Sn atoms. Thus, they scatter the lattice phonons and reduce the thermal conductivity. On the other hand, electrical conductivity is believed to be more constrained to the cage and not much affected by rattling.

$\text{Ba}_6\text{Ge}_{25}$ undergoes a two-step first order structural phase transition at temperatures 215 and 180 K.^{5,6} The structural phase transition is accompanied by dramatic change of transport properties. Above the transition it shows a metal-like conductivity with fairly large value for this class of compounds. At the phase transition this behaviour is profoundly changed; resistivity abruptly increases, then slowly rises with lowering the temperature and saturates at low temperatures. The Hall coefficient smoothly decreases with decreasing the temperature and is not remarkably affected by the phase transition. Magnetic susceptibility is negative and temperature independent above and abruptly decreases at the phase transition similarly to the thermopower.^{5,6} It has been observed that hydrostatic pressure suppresses the phase transition.⁷ The homologue clathrate $\text{Ba}_4\text{Na}_2\text{Ge}_{25}$,⁸ with smaller lattice parameter, does not undergo a phase transition and shows typical metal-like behaviour.⁶ At low temperatures both clathrates experience superconducting transitions.⁷

In this article we consider the electronic band structure of the compounds and the influence of the structural phase transition on the electronic band structure as well as the possible consequences on the transport properties. In Section II some structural details are considered. De-

tails of the calculations are described in Section III. The results and the discussion are presented in Section IV. Finally, the summary and the conclusions are given in Section V.

II. STRUCTURE

The structure of $\text{Ba}_6\text{Ge}_{25}$ belongs to the space group $P4_132$ (No. 213). There are 124 atoms in the unit cell. All the structural details can be found in Ref. 1,8,9,10. Thorough description of the structure can also be found in Ref. 11,12 on structurally similar Sn clathrates. Germanium atoms form the framework which defines three different types of cages filled with barium atoms. The main building blocks are distorted germanium pentagon-dodecahedra with Ba1 atoms inside. They form a chiral network with large cavities, where Ba2 and Ba3 atoms are placed. In the $\text{Ba}_4\text{Na}_2\text{Ge}_{25}$, two sodium atoms are randomly distributed in three Ba2 sites per formula unit. In total, 17 of 25 germanium atoms per formula unit are four-fold coordinated by other germanium atoms. The remaining 8, usually denoted as Ge3 and Ge5, are three-fold coordinated. The average distance between germanium atoms ($\sim 2.54 \text{ \AA}$) is somewhat larger than for Ge in diamond type structure ($\sim 2.45 \text{ \AA}$) and the angles are distorted. Typical nearest distance between barium and germanium atoms is around 3.5 \AA . The nearest distance between barium atoms is around 4.70 \AA for Ba2-Ba3 in undistorted structure (see also Ref. 10).

Due to highly aspherical electron density deduced from X-ray diffraction data, split positions for Ba2 and Ba3 atoms are assumed. The most pronounced effect at the structural phase transition is the increase of the atomic displacement parameter for Ba2, and somewhat less for Ba3 atom.^{9,10} It is believed that below the phase transition Ba2 and Ba3 atoms are actually locked in the split sites. However, since no superstructure is observed, they should be randomly distributed among split sites.

The germanium cage also undergoes modifications at the phase transition and there is not only a difference between the room temperature and the low temperature structure, but also the variation with temperature through the whole temperature range.¹⁰

III. COMPUTATIONAL DETAILS

Band structure calculations were performed within Local Density Approximation (LDA) using Linear Muffin Tin Orbital (LMTO) method in Atomic Sphere Approximation (ASA) with combined correction terms taken into account.^{14,15} Scalar relativistic version was used with von Barth-Hedin exchange-correlation potential.¹⁶

The calculations for the room- and the low-temperature structural data for $\text{Ba}_6\text{Ge}_{25}$ were performed. The atomic parameters for different models used in calculations are given in Table I. The barium atoms were placed in their average positions within higher symmetry model, i.e., space group $P4_132$. In $\text{Ba}_4\text{Na}_2\text{Ge}_{25}$, the random distribution of the Na and Ba atoms at Ba2 site was neglected and the calculations were performed for lower symmetry model, namely, group $P4_12_12$ (No. 92), with sodium atoms at one of the $8b$ symmetry sites.

The calculations with Ba2 and Na atoms shifted from their average positions in the original space groups (No. 213 and No. 92, respectively) were performed using lower symmetry models in space groups $P2_13$ (No. 198) and $P4_1$ (No. 76), respectively. In this way the assumed randomness of the locking was not considered.

Most of the results presented in this work were obtained from self-consistent calculations on $12 \times 12 \times 12$ k-space mesh. For the detailed band structure around Fermi level the calculations were performed for the $16 \times 16 \times 16$ mesh. The values of the DOS at the Fermi level for these cases showed corresponding variations of about 1 eV^{-1} per unit cell. The total energy was negligibly affected by this change of the mesh size.

The atomic sphere radii were determined so that their overlap was minimised. This resulted in the radii of about 1.5 \AA (2.9 a.u.) for germanium and 2.5 \AA (4.8 a.u.) for barium atoms. It is worth to note that, as the radii of germanium spheres are rather small, germanium p -states extend far beyond the sphere boundaries. The large part of these states, so called "tails," reside in the neighbouring barium spheres. This should be taken into account when considering barium and germanium charges which are defined as the integrals of the electron density over the corresponding sphere. They are clearly identified in the empty spheres of hypothetical $\square_6\text{Ge}_{25}$, where the barium atoms are replaced by the empty spheres of the same radii. In this case a high electron density near the boundary can be observed which diminishes toward the center of the empty sphere. Because of the large barium spheres, also the states of f -symmetry were used in the expansion of the wave function. In the germanium spheres the wave function was expanded up to the states of d -symmetry.

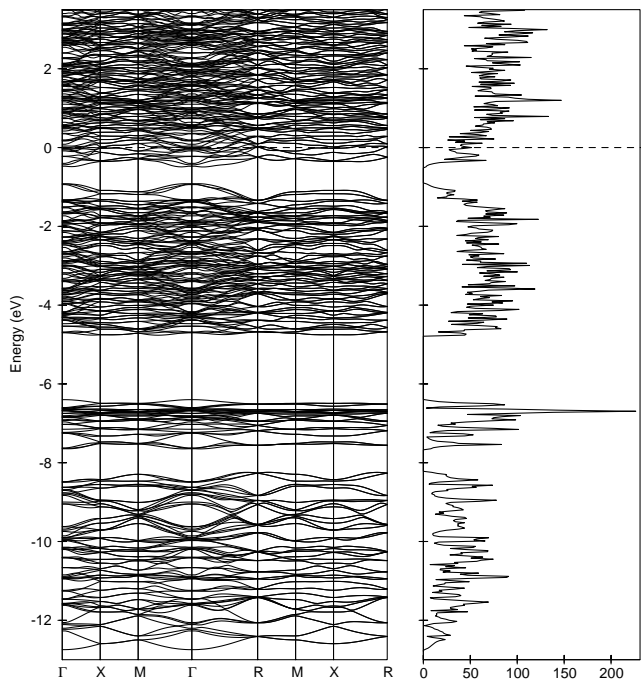


FIG. 1: The electronic band structure and the density of states for $\text{Ba}_6\text{Ge}_{25}$ in the low temperature structure at 10 K with Ba atoms in the average positions within space group $P4_132$.

IV. RESULTS AND DISCUSSION

Here we present and discuss the results for the low temperature structure of $\text{Ba}_6\text{Ge}_{25}$ at 10 K, first with Ba atoms in the average sites. We focused the analysis on the density of states and the bonding properties between the barium atoms and the germanium cage. No distinctive qualitative difference in the DOS between the room and the low temperature structures within higher symmetry model was found. Further, we investigated the effects of shifting the barium atoms toward split positions on the band structure. This was done within the low temperature structure, because there the split positions are the most distant and the locking of the barium atoms is assumed. Finally, the results for the $\text{Ba}_4\text{Na}_2\text{Ge}_{25}$, which does not undergo phase transition, are discussed. In particular, the influence of the sodium on the band structure is examined in comparison with barium.

A. Electronic band structure and density of states

The electronic band structure with its density of states calculated for $\text{Ba}_6\text{Ge}_{25}$ in the low temperature undistorted structure are shown in Fig. 1. The overall picture is similar for the room temperature structure. Due to the large number of atoms in the unit cell there is a large number of bands and a complex electronic band structure.

TABLE I: Wyckoff positions splitting from the group No. 213 in its subgroups.¹³ The average structure of Ba₆Ge₂₅ belongs to the space group $P4_132$ (No. 213). The values for the atomic coordinates were taken from Ref. 1,10. Shifting the Ba2 atom toward one of the split positions of Ba4 site demands lowering the symmetry to the space group $P2_13$ (No. 198). For Ba₄Na₂Ge₂₅ (atomic coordinates were taken from Ref. 8) the symmetry had to be lowered to the group $P4_12_12$ (No. 92) so that Na atoms could be orderly placed on Ba2 sites. Shifting the Ba or Na from Ba2 site demands lowering the symmetry to the space group $P4_1$ (No. 76).

Sites	No. 213		No. 198		No. 92		No. 76		
Ge1 Ge5 Ge6 Ba4 (Na) ^a	24e	x, y, z	12b	x, y, z	8b	x, y, z	4a	x, y, z	
						8b	z+7/8, x+3/4, y+3/8	4a	-x+1/2, y+1/2, -z+1/4
				12b	y+3/4, x+1/4, -z+1/4			4a	z+7/8, x+3/4, y+3/8
						8b	y+1/4, z+5/8, x+1/8	4a	-z-3/8, x+1/4, -y-1/8
Ba2 (Na) Ge4	12d	1/8, y, y+1/4	12b	1/8, y, y+1/4	8b	7/8, y+1/2, y+1/8	4a	7/8, y+1/2, y+1/8	
						4a	y+3/4, y+3/4, 0	4a	-3/8, y, -y+1/8
Ba1 Ge2, Ge3	8b	x, x, x	4a	x, x, x	8b	x+3/4, x+1/2, x+7/8	4a	y+3/4, y+3/4, 0	
				4a	-x+3/4, -x+3/4, -x+3/4			4a	x+3/4, x+1/2, x+7/8
Ba3	4a	3/8, 3/8, 3/8	4a	3/8, 3/8, 3/8	4a	1/8, 7/8, 1/4	4a	-x-1/4, x, -x-5/8	
							4a	1/8, 7/8, 1/4	

^aSplit positions of the Ba2 and Na.

In Fig. 2 the l -projections of DOS in germanium atomic spheres are shown: Ge in diamond structure, hypothetical Ge-graphite, $\square_6\text{Ge}_{25}$, and Ba₆Ge₂₅ compounds are compared. In the DOS, s -, sp -, and p -bonding regions can be recognised in filled and empty clathrate similar to those in Ge-diamond or graphite. This similarity is to be expected since locally 17 of 25 germanium atoms per formula unit are four-fold coordinated (4b) and form covalent sp^3 -like bonds, like in the diamond structure. The other 8 germanium atoms are three-fold bonded (3b) more like in graphite structure. The total width of the bonding region is about 0.9 eV narrower in the empty and filled clathrates. The fundamental gap between bonding and anti-bonding region is larger in $\square_6\text{Ge}_{25}$ than in the diamond structure by the same amount of 0.9 eV and there appears a gap between sp - and p -like bands in the valence region. These features are common for the other Ge and Si clathrates (e.g., Ref. 17). The appearance of the gap in the valence region by its contraction was associated with the 5-ring patterns (pentagons) of germanium or silicon atoms,^{18,19} but there was also some criticism of the idea.²⁰ According to the latter, the small angular distortion of the tetrahedrally bonded framework may also play an important role. While for Ge clathrates of type I and II an overlap of the s - and sp -region is observed,¹⁷ here one can see a clear separation. One should keep in mind that in Ba₆Ge₂₅ structure, in contrast to the clathrates I and II, there are three bonded germanium atoms. However, the band structure calculation on hypothetical Ge-graphite, where all germanium atoms are three-fold coordinated, did not reveal pronounced tendency toward such a separating of the s - and sp -regions, as seen in Fig. 2.

The main difference in the site projected DOS for germanium atomic spheres between the empty and the filled clathrate is the reduction of the gap between bonding and

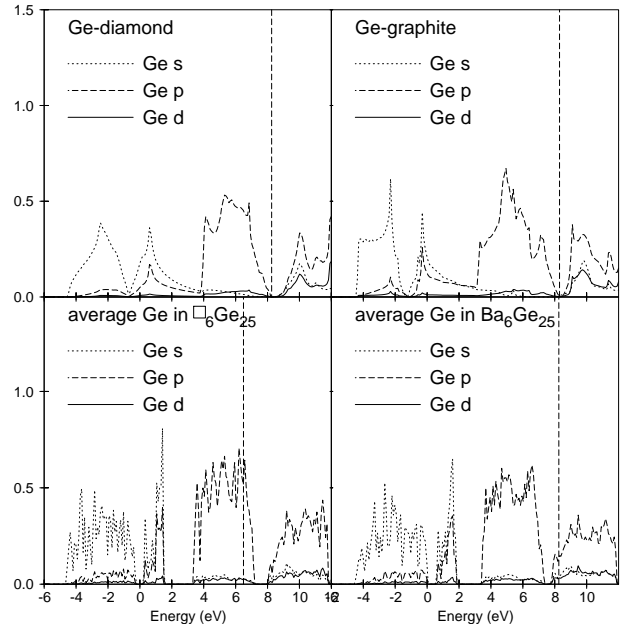


FIG. 2: Projected density of states from Ge atomic spheres in Ge-diamond, hypothetical graphite structures, Ba₆Ge₂₅ and $\square_6\text{Ge}_{25}$. For the clathrate compounds, the average contribution from all germanium is shown.

anti-bonding region in the filled clathrate. This immediately shows the importance of barium atoms not only as the pure electron donors to the conduction band formed of germanium anti-bonding states.

The three-bonded germanium atoms, six Ge5 and two Ge3, form a distorted cube around Ba3. Ba2 atoms lie on the lines passing from the central Ba3 through the cube faces formed by three Ge5 and one Ge3 atom. In this way they form a large octahedron around Ba3. The closest

TABLE II: Total charges in the atomic spheres and their radii for $\text{Ba}_6\text{Ge}_{25}$ and $\square_6\text{Ge}_{25}$.

At. Sphere	$\text{Ba}_6\text{Ge}_{25}$	$\square_6\text{Ge}_{25}$	difference	AS radius (a.u.)
Ba1, $\square 1$	4.613	2.853	1.760	4.7175
Ba2, $\square 2$	3.474	1.864	1.610	4.6919
Ba3, $\square 3$	3.711	1.776	1.935	4.8720
Ge1	3.520	3.462	0.058	2.8663
Ge2	3.821	3.805	0.016	2.9607
Ge3(3b)	3.536	3.403	0.133	2.9829
Ge4	3.613	3.619	-0.006	2.8728
Ge5(3b)	3.436	3.315	0.121	2.8675
Ge6	3.559	3.499	0.060	2.8648

distances are between Ba2 and Ge3, 3.35 Å, and Ba3 and Ge5 3.38 Å. Ge3 atoms are somewhat more distant from Ba3, at 3.89 Å. This environment and the nature of the bonds between Ba3, Ge3, Ge5, and Ba2 should be the key to understand the physical properties of the compound and its phase transition.¹⁰

Let us consider the charges in the atomic spheres. As mentioned in Section III, there is a large contribution of germanium states in the oversized barium spheres. This can be seen in Table II in the column for the charges of empty clathrate, $\square_6\text{Ge}_{25}$. The large charges in the empty spheres are coming from the tails of germanium states. The highest value is in $\square 1$. This is expected because $\square 1$ has the closest Ge neighbours forming distorted pentagon-dodecahedron. Despite of the fact that $\square 3$ has the largest sphere, relatively smaller charge is found inside due to the fewer Ge neighbours. For three-bonded germanium atoms it can also be noted that they have somewhat smaller charges inside their spheres in comparison to the four-bonded germanium, although e.g., Ge3 has the largest atomic sphere from all germanium atoms. Among germanium atoms, three-bonded Ge3 and Ge5 have the largest increase of the charge upon inclusion of barium atoms. This is in accord with the expectation of Zintl concept, namely, that three-bonded germanium atoms accept an electron from barium atoms to form the lone electron pairs. However, because of the small germanium spheres the absolute value of the difference is not so pronounced. Among barium spheres, the largest increase of the charge, in comparison to the corresponding empty spheres, undergoes the Ba3 sphere. We interpret this as the influence of the lone pairs, reflected in the Ba3 sphere as the tails from neighbouring three-bonded germanium atoms. This is illustrated in Fig. 3 where the differences of the l -projected radial charge densities in the several atomic spheres are shown. The large electron density near the boundary of Ba3 atomic sphere may be associated with the lone electron pairs of the neighbouring three-bonded germanium atoms. It was also shown by electron localisation function (ELF) analysis that these lone pairs are situated around Ba3 site.¹⁰ The oscillating part of the density, i.e., its difference shown in Fig. 3, may be interpreted as more atomic-like barium states. The biggest contribution comes from the states

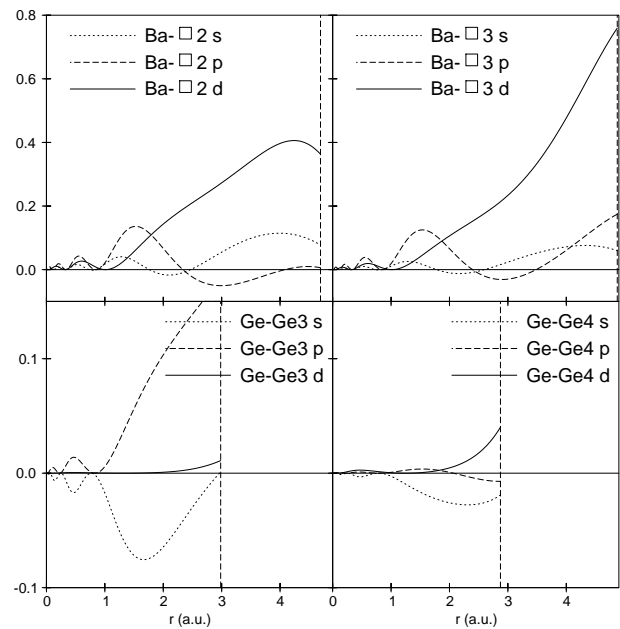


FIG. 3: Electron density difference between filled and empty clathrate in particular atomic spheres.

of d -symmetry.

We conclude that there is only a small charge transfer from barium to the cage, just in agreement with conclusion made for $\text{Ba}_8\text{Ga}_{16}\text{Ge}_{30}$ in Ref. 21, with difference, that here all the arguments point out that a considerable amount of the electron charge remains in the states with significant barium character. This is in contrast to the situation reported for K_8Ge_{46} in Ref. 22 where the authors conclude complete charge transfer from potassium atom to the frame. Both of these cited results were critically re-considered and charge transfer redefined in the recent paper.²³ However, as may be seen in Fig. 3, the large amount of the charge in the barium spheres resides near the boundaries, so that it may be said that the conduction electrons are more constrained to the cage.

In the band structure calculations for the similar K_6Sn_{25} and $\text{K}_6\text{Sn}_{23}\text{Bi}_2$ compounds, a lifting of the three bands, originated only from three-bonded tin atoms, from the top of the valence region was found and ascribed to the interaction of the lone pairs formed by three-bonded tin atoms.¹² But, as was pointed out there, in $\text{Ba}_6\text{Ge}_{21}\text{In}_4$ this characteristic is absent due to a smaller spatial extension of germanium orbitals. We did not notice significant difference of DOS between three-bonded (Ge3, Ge5) and four-bonded germanium atomic spheres. However, as discussed above, we expect that the lone electron pair states mostly reside as tails in $\square 3$ atomic sphere. Therefore one might expect their contribution to the DOS in $\square 3$ sphere in $\square_6\text{Ge}_{25}$. Indeed, we find a peak in DOS on the top of the unoccupied valence region (Fig. 4) appearing only in $\square 3$ sphere. This peak remains in the filled clathrate, i.e., in Ba3 sphere, what can also be seen in Fig. 4. For Ba2 and Ba3 spheres a

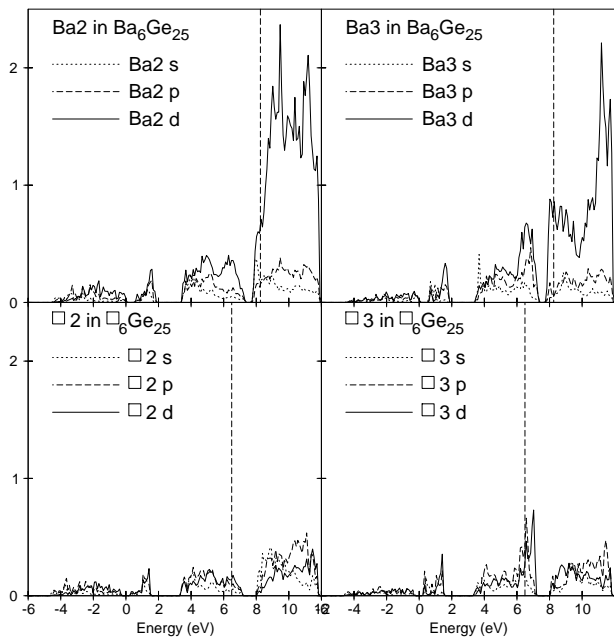


FIG. 4: The projected density of states from atomic spheres of Ba2 and Ba3 in $\text{Ba}_6\text{Ge}_{25}$ and the equivalent empty spheres of $\square 2$ and $\square 3$ in $\square_6\text{Ge}_{25}$.

large increase of DOS, compared to the empty $\square 2$ and $\square 3$ spheres, in the region around the Fermi energy is found. The number of states is increased and this suggests that the barium states participate in the conduction band formation.

This is in contrast to the results for the $\text{Ba}_8\text{Ga}_{16}\text{Ge}_{30}$ clathrate²¹ where the inclusion of barium atoms inside the Ga-Ge cage left the band structure almost intact. This is also different to the cases of some Si clathrates²⁴ where the main effect of the inclusion of alkali metal was shifting of the particular state at the bottom of the conduction band, but still predominantly of the cage-like character so that it was possible to neglect the overlap of the orbitals of guest atoms with host-cage. Here, however, the distances between the barium and germanium atoms are shorter and stronger hybridisation may be expected.

Another important feature of DOS is that it shows a peak just at the Fermi level (Fig. 5). Its value is around 50 states/eV per unit cell in the low temperature structure. The largest contributions come from barium atomic spheres mainly with d -symmetry and from p -states in germanium atomic spheres. The shape of the DOS coming from barium and germanium spheres follows closely each other. This indicates a strong hybridisation of barium and germanium states. The contribution from Ba1 spheres is significantly lower than that from Ba2 and Ba3 spheres, although Ba1 has the nearest Ge neighbours. This complies with the assumption that the Ba2 and Ba3 atoms with the surrounding three-bonded germanium atoms determine the most unusual properties of the system. It is quite interesting that the similar peak

of the DOS at the Fermi energy was found for $\text{Ba}_8\text{Si}_{46}$ clathrate^{18,19} as well. In that case also the relatively shorter distances between the barium and silicon atoms were found ($\sim 3.3\text{-}3.5$ Å). We have also performed calculation for $\text{Ba}_6\text{Si}_{25}$.²⁵ The lattice parameter is smaller compared to the Ge clathrate and the fundamental gap disappears completely but the peak in the DOS at the Fermi level with strong contribution of the states with d -symmetry coming from the barium atomic spheres remains (Fig. 5). It is also interesting that the subband-gap between s - and sp - regions (not shown in the Fig. 5) appears in the $\text{Ba}_6\text{Si}_{25}$ as well.

For a better understanding of the above results, i.e., the role that is played by barium states, we have performed the calculation with barium atoms only, $\text{Ba}_6\square_{25}$, without the Ge framework. The distances between Ba2 and Ba3 atoms of about 4.70 Å are comparable to the distances between atoms in Ba bcc structure with 4.34 Å. The calculation showed the dominant contribution of d -symmetry states at the Fermi level. The s -states are split into bonding and the anti-bonding regions. The bonding states lie below Fermi level and anti-bonding above, so that they do not give significant contribution to the DOS at the Fermi level. The tails of the barium d -states in the empty germanium spheres are of s - and p -symmetry, so that the appreciable overlap of these states with germanium s - and p -states in the filled clathrate might be expected. Concerning the relative energy parameters of the barium and germanium muffin-tin orbitals, they showed qualitative agreement with the values used for the atomic orbitals in LCAO calculations.²⁶ All these facts suggest that the appearance of the barium d -states and their hybridisation with germanium p -states at the Fermi level is quite plausible.

The possible importance of the hybridisation of the Ba $5d$ states with Si cage was also pointed out for $\text{Ba}_8\text{Si}_{46}$.¹⁸ The results of the experiment with ultrahigh-resolution photoemission spectroscopy for $\text{Ba}_8\text{Si}_{46}$ suggest even stronger hybridisation of Ba and Si states than obtained in LDA calculation.²⁷ NMR experiments on this compound could be interpreted if strong contribution of Ba d -states to the DOS at the Fermi energy is assumed.²⁸

B. Band structure near the Fermi level versus Ba2 shift

The presence of the peak in the DOS at the Fermi level suggests a possible instability of the system. Since there are strong indications of locking of Ba2 atoms at the phase transition, as mentioned in Section II, we investigated the modifications of the band structure due to the shifting of Ba2 atoms within the low temperature structure.

The most interesting effect of this shifting of Ba2 atoms, performed as explained in Section III, is the splitting of the peak at the Fermi level and, consequently, the reduction of DOS. The effect was found to be the most

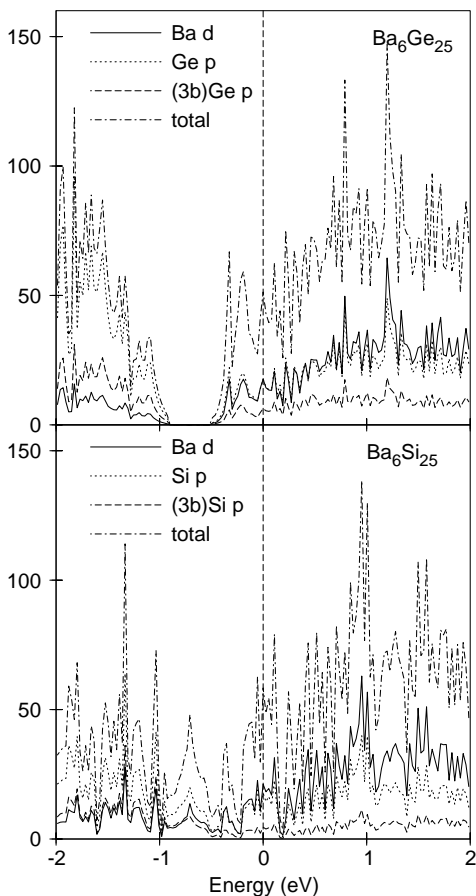


FIG. 5: Contribution to DOS from all Ba d -states, all Ge p -states and all three-bonded Ge p -states per formula unit. The total DOS is also shown. In the figure below the same is shown for the case of $\text{Ba}_6\text{Si}_{25}$, with Si atoms instead of Ge.

pronounced with Ba2 at 80% distance from the higher symmetry position toward the experimental split position. In Fig. 6, the band structure together with the DOS in the close vicinity of the Fermi level for this structure is compared with the higher-symmetry (average) structure. The effect may be considered as a band Jahn-Teller effect, though in the band structure along the symmetry directions no obvious removing of the degeneracy is observed. The equivalent scenario was proposed for some other compounds with somewhat similar metal-insulator transition.²⁹ The conventional Jahn-Teller effect was considered also for some other clathrates.^{24,30,31}

The total energy was also compared for shifted positions. The minimum was found to be at the off average position. The potential energy surface for Ba atoms showed binding stronger than expected, but the variation of the total energy with respect to the shifting of atoms is known not to be highly accurate within the atomic sphere approximation. That is also the reason why the structure optimization was not performed.

One has to be careful with the interpretations, especially because the whole framework is slightly changing

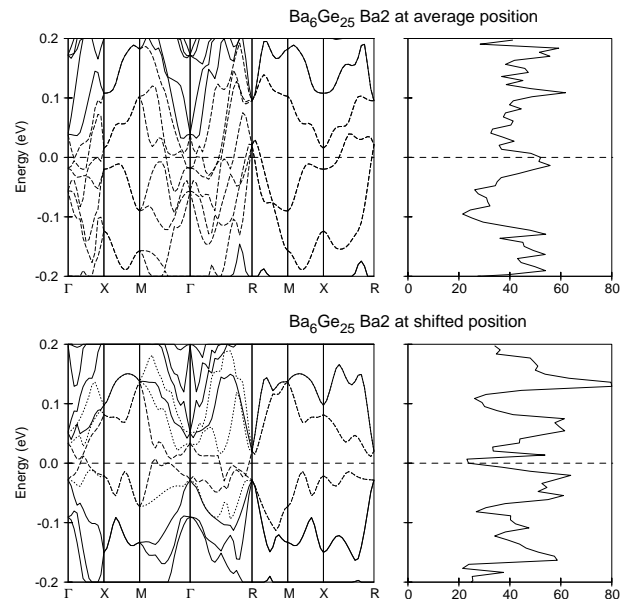


FIG. 6: Electronic band structure and the density of states around the Fermi energy for the Ba2 at the average position and at 80% toward the split site in $\text{Ba}_6\text{Ge}_{25}$. Dashed lines designate the bands that are crossing the Fermi level.

with the temperature and is strongly disturbed during the phase transition.¹⁰ As mentioned before, we did not notice a qualitative difference in the DOS between the room temperature and the low temperature higher symmetry structures. For both of them the peak at the Fermi level is found. The splitting of the peak when Ba2 atom is shifted toward one of the split positions indicates that the locking of barium atoms might be the most important process at the phase transition. If we assume that at the phase transition this locking of barium atoms occurs then the reduction of the DOS at the Fermi level is in a qualitative agreement with the observed decrease of magnetic susceptibility. The decrease of the value of DOS is found to be around 25 eV^{-1} per unit cell which corresponds to a drop of the Pauli susceptibility of $2.08 \times 10^{-4} \text{ cm}^3/\text{mol}$ per formula unit that agrees in order of magnitude with the observed one.^{5,6} Moreover, the area of the Fermi surface is reduced because there are less bands crossing the Fermi level, what can also be seen in Fig. 6. As a consequence, electrical conductivity is expected to be lower and this is also in accord with the experimental observation. It should be emphasised that we did not take into account the effect of the disorder of locked barium atoms. However, due to a very short electron mean free path, which is much smaller than the unit cell parameter, as estimated from experiments and a simple free electron model,⁶ the barium disorder effects should not reflect themselves in the transport properties. The same argument may be applied to understand experimental Hall coefficient results, i.e., the electrons might not be able to close the trajectory on the Fermi surface and therefore the Hall coefficient might not be strongly influenced

by the phase transition. The absolute value of DOS at the Fermi level is in agreement with the low temperature specific heat measurements.⁷ If we assume the locking of barium atoms at low temperatures and take the corresponding value of DOS of 25 eV^{-1} at the Fermi level, we obtain $\gamma = 15 \text{ mJ/molK}^2$ per formula unit. The experimental value is 21 mJ/molK^2 per formula unit. For the $\text{Ba}_4\text{Na}_2\text{Ge}_{25}$, discussed in the next section, we obtain 29 mJ/molK^2 per formula unit in comparison with the experimental 33 mJ/molK^2 per formula unit. The measurements of the variation of superconducting transition temperature under pressure show that T_c is increased 16 times, from the value of 0.24 K at zero pressure, as the structural phase transition is suppressed. Introducing the values of DOS for higher and lower symmetry structure in the McMillan expression for T_c ³² provides the ratio of 21, in a relatively good agreement with the observed one.

C. The results for $\text{Ba}_4\text{Na}_2\text{Ge}_{25}$

The total band structure for $\text{Ba}_4\text{Na}_2\text{Ge}_{25}$ is qualitatively similar to that found for $\text{Ba}_6\text{Ge}_{25}$. The Fermi level is shifted downwards because there are less electrons and the gap between bonding and anti-bonding region is narrower since the lattice parameter is smaller compared to $\text{Ba}_6\text{Ge}_{25}$. The peak of DOS at the Fermi level is also found.

In order to examine the influence of the sodium on the band structure, we performed a calculation on a fictitious $\text{Ba}_4\text{Na}_2\text{Ge}_{25}$ compound and compare it with $\text{Ba}_4\text{Na}_2\text{Ge}_{25}$. The inclusion of sodium atoms introduces a lowering of the bands at the beginning of the conduction band together with the most upper parts of the valence bands, so that the fundamental gap has nearly the same value. The conduction bands are modified. Although some similarities may be observed, rigid-band model could hardly be applied. In the valence region, however, apart from the bands just below the fundamental gap, near Γ point, the band structures are almost identical. Introduction of sodium does not influence the bonding states of germanium. The l -projected DOS in sodium atomic spheres are shown in Fig. 8, and compared with the pertinent empty sphere. In the sodium sphere a peak of mainly s -symmetry at the Fermi level is found, where the modifications of the band structure, considered above, is observed.

We have also performed a calculation on $\text{Ba}_4\text{Ba}_2\text{Ge}_{25}$, where we have inserted barium instead of sodium atoms and kept the same symmetry and the structure. It is interesting that no shifting of the conduction band is observed. However, the band structure undergoes stronger changes than in the case of sodium. Even the valence region, i.e., bonding germanium states, is significantly affected. The l -projected DOS in the barium spheres, as in $\text{Ba}_6\text{Ge}_{25}$, discovers the appearance of the states of d -symmetry (Fig. 8). The large contribution of d -symmetry states are present around and above the Fermi level, in

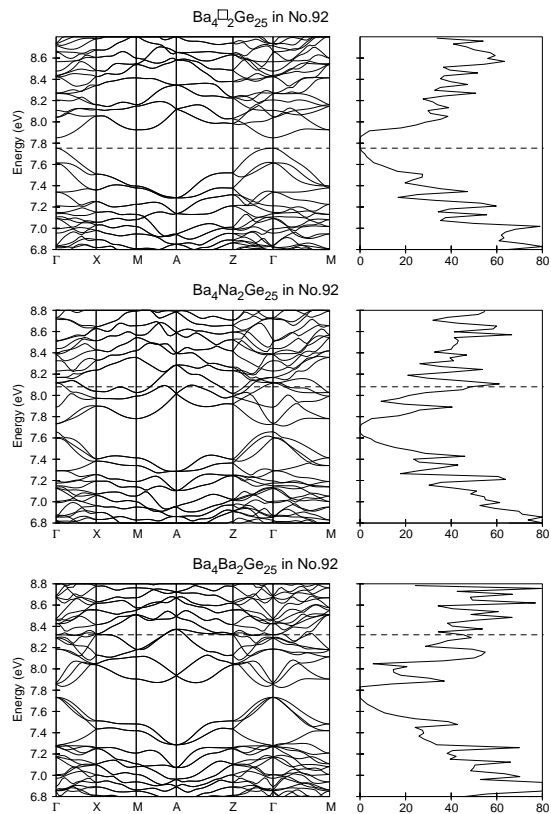


FIG. 7: Comparison of the band structures around the Fermi level of the fictitious $\text{Ba}_4\text{Na}_2\text{Ge}_{25}$, $\text{Ba}_4\text{Na}_2\text{Ge}_{25}$, and $\text{Ba}_4\text{Ba}_2\text{Ge}_{25}$ with same structure and symmetry as $\text{Ba}_4\text{Na}_2\text{Ge}_{25}$.

contrast to the sodium and the empty spheres, where their contribution is small.

The electron charges, projected on the states of particular l -symmetry, in the sodium, barium, and empty spheres for corresponding compounds are given in the Table III. Since in the empty spheres only the tails from germanium states are present, the difference to the spheres of sodium and barium should give the contribution of more atomic-like states. In the sodium sphere, the charge is mainly in the states of s -symmetry, but comparable contributions are found in the states of p - and somewhat less in d -symmetry states. Due to the change of the potential in the sodium sphere in comparison with empty one, it is hard to disentangle the contribution coming from germanium tails. The values, however, indicate hybridisation of sodium s - and p -states with germanium states, although not so strong as in the case of barium in $\text{Ba}_4\text{Ba}_2\text{Ge}_{25}$, where a distinctively large contribution of d -symmetry states in the barium sphere is found, which again points to the strong hybridisation of barium d -states with germanium p -states.

A shifting of sodium atoms to one of the split positions did not produce such a splitting of the band structure as in the case of $\text{Ba}_6\text{Ge}_{25}$, although some reduction of DOS is observed.

TABLE III: The electron charge in the particular Ba, Na, and \square atomic sphere of $\text{Ba}_4\text{Na}_2\text{Ge}_{25}$, $\text{Ba}_4\square_2\text{Ge}_{25}$, and $\text{Ba}_4\text{Ba}_2\text{Ge}_{25}$, decomposed in the states of particular orbital angular momentum quantum number. The calculations for all compounds were performed within the same space group (No. 92) with the same structure parameters. Ba2, Na, and \square atomic spheres are all of the same radius of 4.59 a.u. and are equivalent to the Ba2 site in the $\text{Ba}_6\text{Ge}_{25}$ in the original space group No. 213.

At.sphere	$\text{Ba}_4\text{Na}_2\text{Ge}_{25}$				$\text{Ba}_4\square_2\text{Ge}_{25}$				Difference			
	<i>s</i>	<i>p</i>	<i>d</i>	<i>f</i>	<i>s</i>	<i>p</i>	<i>d</i>	<i>f</i>	<i>s</i>	<i>p</i>	<i>d</i>	<i>f</i>
Ba2	0.53	0.76	1.52	0.43	0.49	0.76	1.51	0.43	0.04	0.00	0.01	0.00
Na, \square	0.65	0.89	0.71	0.39	0.34	0.65	0.58	0.37	0.31	0.24	0.13	0.02
	$\text{Ba}_4\text{Ba}_2\text{Ge}_{25}$				$\text{Ba}_4\square_2\text{Ge}_{25}$							
Ba_2,\square^a	0.55	0.76	1.53	0.43	0.34	0.65	0.58	0.37	0.21	0.11	0.95	0.06

^aThese correspond to the Na site in $\text{Ba}_4\text{Na}_2\text{Ge}_{25}$

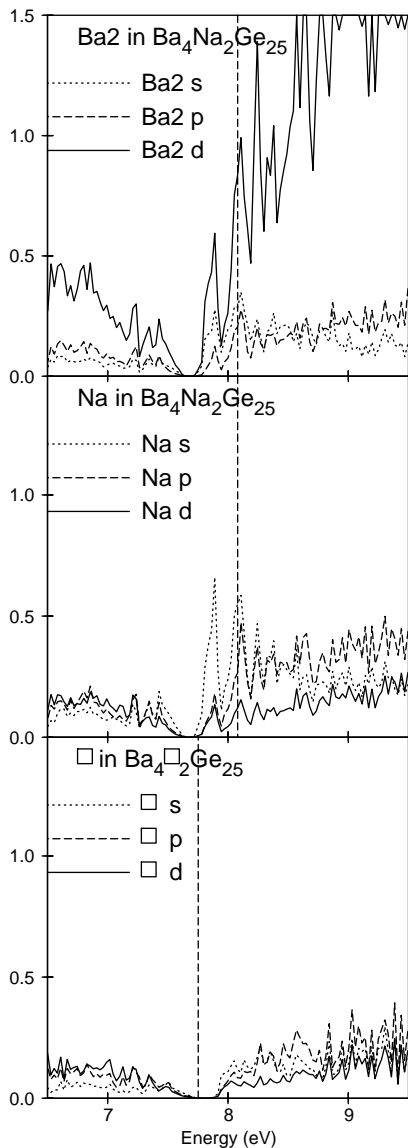


FIG. 8: The *l*-projected density of states from Ba2 and Na atomic spheres in $\text{Ba}_4\text{Na}_2\text{Ge}_{25}$ and \square sphere, equivalent to the Na sphere, in $\text{Ba}_4\square_2\text{Ge}_{25}$. They all correspond to the Ba2 site in $\text{Ba}_6\text{Ge}_{25}$ in the original space group No. 213.

V. SUMMARY AND CONCLUSION

We have performed LDA band structure calculations for the two clathrates, $\text{Ba}_6\text{Ge}_{25}$ and $\text{Ba}_4\text{Na}_2\text{Ge}_{25}$, using LMTO method within the atomic sphere approximation. The overall band structure reveals similarities with Ge in diamond type structure and the comparison with empty Ge cage shows very similar structure in the bonding region. However, the conduction bands, in particular at the Fermi level, have a strong contribution of barium states. The analysis of the *l*-projected DOS shows that these states are of strong *d*-symmetry character. The calculations yield the peak of the DOS at the Fermi level that hints on the structural instabilities of the system. In $\text{Ba}_6\text{Ge}_{25}$, shifting of Ba2 atoms, which have the largest and the most aspherical atomic displacement parameter, toward one of the experimentally deduced split positions splits the peak and reduces the DOS. The splitting of the peak at the Fermi level, due to the shifting of Ba2 atoms and corresponding symmetry lowering, may therefore be considered as the band Jahn-Teller effect. Barium in $\text{Ba}_6\text{Ge}_{25}$ clathrate can not be considered as the electron donor only and this compound does not fit into the simple concept of PGEC. In the case of $\text{Ba}_4\text{Na}_2\text{Ge}_{25}$, the shifting of sodium atoms to one of the split positions does not produce such a pronounced tendency toward splitting the peak of DOS. If the locking of Ba2 atoms in $\text{Ba}_6\text{Ge}_{25}$ at the phase transition is assumed, the reduction of DOS at the Fermi level is in the agreement with experimentally observed abrupt decrease of the magnetic susceptibility and with the observed variation of superconducting transition temperature with pressure. It may qualitatively account for the observed reduction of the electrical conductivity. The specific heat coefficient γ obtained from the low temperature specific heat measurements is also in agreement with the calculated value of DOS at the Fermi for $\text{Ba}_6\text{Ge}_{25}$ with barium atoms locked, and for $\text{Ba}_4\text{Na}_2\text{Ge}_{25}$ in the average structure.

Acknowledgments

Cabrera.

We wish to acknowledge useful discussions with P. Fulde, S. Paschen, F. M. Grosche and W. Carrillo-

-
- ¹ W. Carrillo-Cabrera, J. Curda, H. G. von Schnering, S. Paschen and Yu. Grin, *Z. Kristallogr. NCS* **215**, 207 (2000).
² S.-J. Kim, S. Hu, C. Uher, T. Hogan, B. Huang, J. D. Corbett and M. G. Kanatzidis, *J. Solid State Chem.* **153**, 321 (2000).
³ H. Fukuoka, K. Iwai, S. Yamanaka, H. Abe, K. Yoza and L. Häming, *J. Solid State Chem.* **151**, 117 (2000).
⁴ G. S. Nolas, G. A. Slack and S. B. Schujman, *Semiconductors and Semimetals* **69**, 255 (2001).
⁵ S. Paschen, V. H. Tran, M. Baenitz, W. Carrillo-Cabrera, R. Michalak, Yu. Grin and F. Steglich, in *Proceedings of XIX International Conference on Thermoelectrics*, edited by D. M. Rowe (Babrow Press Wales, UK, 2000), p. 374.
⁶ S. Paschen, V. H. Tran, M. Baenitz, W. Carrillo-Cabrera, Yu. Grin and F. Steglich, *Phys. Rev. B* **65**, 134435 (2002).
⁷ F. M. Grosche, H. Q. Yuan, W. Carrillo-Cabrera, S. Paschen, C. Langhammer, F. Kromer, G. Sparn, M. Baenitz, Yu. Grin and F. Steglich, *Phys. Rev. Lett.* **87**, 247003 (2001).
⁸ W. Carrillo-Cabrera, J. Curda, K. Peters, S. Paschen, Yu. Grin and H. G. von Schnering, *Z. Kristallogr. NCS* **216**, 183 (2001).
⁹ S. Paschen, W. Carrillo-Cabrera, M. Baentiz, V. H. Tran, A. Bentien, H. Borrmann, R. Cardoso Gil, R. Michalak, Yu. Grin and F. Steglich, in *MPI-CPfS Development of the Institute and Scientific Report*, MPI-CPfS, Dresden 2000.
¹⁰ W. Carrillo-Cabrera *et al.*, *Phys. Rev. B*, to be submitted.
¹¹ T. S. Fässler and C. Kronseder, *Z. Anorg. All. Chem.* **624**, 561 (1998).
¹² T. F. Fässler, *Z. Anorg. All. Chem.* **624**, 569 (1998).
¹³ U. Müller, *Relations between the Wyckoff positions*, in *International tables for X-ray crystallography*, **A1**, (to be published).
¹⁴ O. K. Andersen, *Phys. Rev. B* **12**, 3060 (1975).
¹⁵ Hans L. Skriver, *The LMTO method*, Springer, Springer series in solid state sciences 41, Berlin 1984.
¹⁶ U. von Barth and L. Hedin, *J. Phys. C* **5**, 1629 (1972).
¹⁷ J. Dong and O. F. Sankey, *J. Phys.: Condens. Matter*, **11**, 6129 (1999).
¹⁸ S. Saito and A. Oshiyama, *Phys. Rev. B* **51**, 2628 (1995).
¹⁹ K. Moriguchi, M. Yonemura, A. Shintani and S. Yamanaka, *Phys. Rev. B* **61**, 9859 (2000).
²⁰ K. Moriguchi, S. Munetoh and A. Shintani, *Phys. Rev. B* **62**, 7138 (2000).
²¹ N. P. Blake, D. Bryan, S. Lattturner, L. Möllnitz, G. D. Stucky and H. Metiu, *J. Chem. Phys.* **114**, 10063 (2001).
²² J. Zhao, A. Buldum, J. P. Lu and C. Y. Fong, *Phys. Rev. B* **60**, 14177 (1999).
²³ T. Nagano, K. Tsumuraya, H. Eguchi and D. J. Singh, *Phys. Rev. B* **64**, 155403 (2001).
²⁴ A. A. Demkov, O. F. Sankey, K. E. Schmidt, G. B. Adams and M. O’Keeffe, *Phys. Rev. B* **50**, 17001 (1994).
²⁵ H. Fukuoka, K. Ueno and S. Yamanaka, *J. Organometallic Chem.* **611**, 543 (2000).
²⁶ W. A. Harrison, *Electronic structure and the properties of solids*, Dover Publications, Inc., New York 1989.
²⁷ T. Yokoya, A. Fukushima, T. Kiss, K. Kobayashi, S. Shin, K. Moriguchi, A. Shintani, H. Fukuoka and S. Yamanaka, *Phys. Rev. B* **64**, 172504 (2001).
²⁸ F. Shimizu, Y. Maniwa, K. Kume, H. Kawaji, S. Yamanaka and M. Ishikawa, *Phys. Rev. B* **54**, 13242 (1996).
²⁹ T. Hagino, T. Tojo, T. Atake and S. Nagata, *Phil. Mag. B* **71**, 881 (1995).
³⁰ V. I. Smelyansky and J. S. Tse, *Chem. Phys. Lett.* **264**, 459 (1997).
³¹ F. Brunet, P. Mélinon, A. San Miguel, P. Kéghélian, A. Perez, A. M. Flank, E. Reny, C. Cros and M. Pouchard, *Phys. Rev. B* **61**, 16550 (2000).
³² W. L. McMillan, *Phys. Rev.* **167**, 331 (1968).